https://doi.org/10.5194/hess-2024-389
Preprint. Discussion started: 21 January 2025
© Author(s) 2025. CC BY 4.0 License.

Hydrology and Earth System Sciences
Discussions

Combining uncertainty quantification and entropy-inspired concepts into a single objective function for rainfall-runoff model calibration

Alonso Pizarro[1], Demetris Koutsoyiannis[2], Alberto Montanari[3]

[1]Escuela de Ingeniería en Obras Civiles, Universidad Diego Portales, Santiago, 8370109, Chile
[2]National Technical University of Athens, Zographou, Athens, 15772, Greece
[3]Department DICAM, University of Bologna, Via del Risorgimento 2, Bologna, 40136, Italy

Correspondence to: Alonso Pizarro (alonso.pizarro@mail.udp.cl)

Abstract. A novel metric for rainfall-runoff model calibration and performance assessment is proposed. By integrating entropy and mutual information concepts as well as uncertainty quantification through BLUECAT (likelihood-free approach), RUMI (Ratio of Uncertainty to Mutual Information) offers a robust framework for quantifying the shared information between observed and simulated stream flows. RUMI's capabilities to calibrate rainfall-runoff models is demonstrated using the GR4J rainfall-runoff model over 99 catchments from various macroclimatic zones, ensuring a comprehensive evaluation. Four additional performance metrics and 50 hydrological signatures were also used for performance assessment. Key findings indicate that RUMI-based simulations provide more consistent and reliable results compared to the traditional Kling-Gupta Efficiency (KGE), with improved performance across multiple metrics and reduced variability. Additionally, RUMI includes uncertainty quantification as a core computation step, offering a more holistic view of model performance. This study highlights the potential of RUMI to enhance hydrological modelling through better performance metrics and uncertainty assessment, contributing to more accurate and reliable hydrological predictions.

1 Introduction

Hydrology has witnessed a growing emphasis on uncertainty quantification, driven by the need to enhance our understanding of catchments and to provide decision-makers with accurate model predictions. This has led to the development of various methodologies aimed at better treating uncertainty, each differing in underlying assumptions, mathematical rigour, and the treatment of error sources (see, e.g., Blazkova and Beven 2002; 2004; Krzysztofowicz 2002). Among these approaches (see Gupta and Govindaraju 2023 for a recent review), we can mention the additive Gaussian and generalised-Gaussian process, the inference in the spectral domain, the time-varying model parameters, and multi-model ensemble methods. Additionally, two philosophies for uncertainty analysis are widely recognised, following formal and informal Bayesian methods (Kennedy and O'Hagan, 2001; Kuczera et al., 2006).

Formal Bayesian methods offer robust frameworks for uncertainty estimation, but they come with their own challenges. Identifying a suitable likelihood function for hydrological models involves careful assumptions that must be transparent and

https://doi.org/10.5194/hess-2024-389
Preprint. Discussion started: 21 January 2025
© Author(s) 2025. CC BY 4.0 License.

understandable to end users (Beven, 2024). Statistical analysis of model errors and likelihood-free approaches have also been proposed. For example, Montanari and Koutsoyiannis (2012) proposed converting deterministic models into stochastic predictors by fitting model errors with meta-Gaussian probability distributions. Similarly, Sikorska, Montanari, and Koutsoyiannis (2015) proposed the nearest neighbouring method to estimate the conditional probability distribution of the error. More recently, Koutsoyiannis and Montanari (2022) introduced a simple method to simulate stochastic runoff responses called Brisk Local Uncertainty Estimator for Hydrological Simulations and Predictions (BLUECAT). BLUECAT is a likelihood-free approach as relies on data only. BLUECAT has recently been applied coupled with climate extrapolations (Koutsoyiannis and Montanari 2022), rainfall-runoff modelling in a variety of different hydroclimatic conditions (Jorquera and Pizarro, 2023), and comparisons with machine-learning methods (Auer et al., 2024; Rozos et al., 2022).

Informal Bayesian methods are more flexible, but they lack statistical rigour. A notable example of a relatively simple approach is the Generalized Likelihood Uncertainty Estimation (GLUE) method introduced by Beven and Binley (1992). GLUE operates within the framework of Monte Carlo analysis coupled with Bayesian or fuzzy uncertainty estimation and propagation. Since its introduction, GLUE has seen widespread application across various fields, including rainfall-runoff modelling (among others). Its popularity is mainly due to its conceptual simplicity and ease of implementation. It can account for all causes of uncertainty, either explicitly or implicitly, and allows for evaluating multiple competing modelling approaches, embracing the concept of equifinality (Beven, 1993). However, GLUE has faced criticism in terms of the subjective decisions required in its application and how these affect prediction limits (informal likelihood function, lacks of maximum likelihood parameter estimation, and omission of explicit model error consideration). This subjectivity might lead to not being formally Bayesian (for that reason, GLUE includes the term "generalized" in its name), leading to possibly statistically incoherent and potentially unreliable parameter and predictive distributions (Christensen, 2004; Mantovan and Todini, 2006; Montanari, 2005; Stedinger et al., 2008). Proponents of GLUE argue that it is a practical methodology for assessing uncertainty in non-ideal cases (Beven, 2006), while critics advocate for coherent probabilistic approaches. This ongoing debate underscores the need to establish common ground between these perspectives. Under various conditions, both Bayesian and informal Bayesian methods can yield similar estimates of predictive uncertainty. Building on previous work (see, e.g., Blasone et al. 2008), researchers have compared GLUE with formal Bayesian approaches using advanced Monte Carlo Markov Chain (MCMC) schemes such as the Differential Evolution Adaptive Metropolis (DREAM, Vrugt et al. 2008). With its advantages over traditional global optimisation algorithms, the DREAM algorithm maintains detailed balance and ergodicity, enabling it to provide an exact Bayesian estimate of uncertainty. Additionally, studies have addressed these questions by assessing the uncertainty in synthetic river flow data using GLUE (see, e.g., Montanari 2005) and introducing open-source software packages such as the CREDIBLE uncertainty estimation toolbox (CURE, Page et al. (2023)), coded in Matlab (https://www.lancaster.ac.uk/lec/sites/qnfm/credible/default.htm, last access: 03/12/2024). CURE includes several methods, among them the Forward Uncertainty Estimation; GLUE; and, Bayesian Statistical Methods.

https://doi.org/10.5194/hess-2024-389
Preprint. Discussion started: 21 January 2025
© Author(s) 2025. CC BY 4.0 License.

In addition to these methods, information theory offers valuable tools for quantifying information in hydrological models. Shannon's (1948) seminal work on information theory introduced measures such as Shannon entropy, which quantifies the expected surprise (or information) in a sample from a distribution of states. Shannon entropy can be extended to joint distributions of multiple variables, including conditional dependencies. In hydrology, Shannon entropy and mutual information have been used to assess the uncertainty in discharge predictions, as demonstrated by Amorocho and Espildora (1973) and Chapman (1986). More recently, Weijs, Schoups, and van de Giesen (2010); Weijs, Van Nooijen, and Van De Giesen (2010); Gong et al. (2013, 2014); Pechlivanidis et al. (2014); Pechlivanidis et al. (2016); Ruddell, Drewry, and Nearing (2019) used information-theoretic objective functions for model evaluation. Despite the challenges associated with accounting for uncertainties and statistical dependencies in time series data, information-theoretic objective functions have proven valuable for streamflow simulations, complementing traditional measures such as the Nash-Sutcliffe efficiency (NSE; Nash and Sutcliffe 1970) and the Kling-Gupta efficiency (KGE; Gupta et al. 2009; Kling, Fuchs, and Paulin 2012).

In this work, we study the combination of likelihood-free (BLUECAT) and information theory approaches for rainfall-runoff modelling over 99 catchments having different hydroclimatic contexts. The latter with the intention to quantify and reduce uncertainty in hydrological predictions. The Ratio of Uncertainty to Mutual Information (RUMI) is proposed as a dimensionless metric to be adopted as objective function for calibration purposes. The target aligns with the twentieth of the twenty-three unsolved problems in hydrology (*20. How can we disentangle and reduce model structural/parameter/input uncertainty in hydrological prediction?*, Blöschl et al. 2019). In detail, the following questions are herein addressed:

a) How can the calibration of deterministic model parameters be improved by using a stochastic formulation of the deterministic model?
b) How can uncertainty resulting from the final stochastic model be incorporated into the calibration process of the deterministic model?

This paper is organized as follows: Section 2 presents the used database (catchments properties and data availability), rainfall-runoff model description, and calibration strategies. Section 3 shows the calibration's and validation's results of RUMI-based simulations (as well as KGE-based ones). Daily runoff simulations as well as hydrological signatures' are considered. Strengths and limitations are discussed in Section 4, and conclusions are at the end.

2 Methods

2.1 Rainfall-Runoff Model

The Modular Assessment of Rainfall-Runoff Models Toolbox (MARRMoT – Knoben, Freer, Fowler, et al., 2019; Trotter et al., 2022) was selected due to its open-source feature and modular structure. Implemented in MATLAB, MARRMoT offers a suite of 47 lumped models for simulating rainfall-runoff processes. Model calibration is conducted using the Covariance Matrix Adaptation Evolution Strategy (CMA-ES) algorithm (Hansen et al., 2003; Hansen and Ostermeier, 1996).

https://doi.org/10.5194/hess-2024-389
Preprint. Discussion started: 21 January 2025
© Author(s) 2025. CC BY 4.0 License.

MARRMoT version 2.1.2, with the GR4J model, was employed for this study. The GR4J model has four parameters and two storage components. Its primary purpose is to represent processes such as vegetation interception, time delays within the catchment, and water exchange with neighbouring catchments (Perrin et al., 2003). MARRMoT's nomenclature for rainfall-runoff models is "m_XX_YY_ZZp_KKs", where XX is the number of the model within MARRMoT, YY is the model name, ZZ is the number of parameters, and KK is the number of storages. As a consequence, the GR4J model following MARRMoT nomenclature is: "m_07_gr4j_4p_2s". For a comprehensive description, readers are directed to the MARRMoT user manual, available at: https://github.com/wknoben/MARRMoT/blob/master/MARRMoT/User%20manual/v2.-%20User%20manual%20-%20Appendices.pdf (last accessed: 03/12/2024).

2.2 Data

99 catchments were selected from the CAMELS-CL database (Alvarez-Garreton et al., 2018) to ensure that only catchments with near-natural hydrological regimes were included (see Figure 1 for location and chosen catchment characteristics). The latter was achieved through eight specific criteria: first, the daily discharge time series, though possibly non-consecutive, had to have less than 25% missing data for the period 1990–2018. Additionally, catchments with large dams were excluded (big_dam = 0). Additionally, catchments with more than 10% of discharge allocated to consumptive uses were excluded (i.e., interv_degree < 0.1 to be considered). Catchments with glacier cover higher than 5% were also excluded (i.e., lc_glacier < 5% to be considered). Furthermore, the selected catchments had less than 5% of their area classified as urban (imp_frac < 5%), and irrigation abstractions did not exceed 20% (crop_frac < 20%). Areas with forest plantations covering more than 20% of the catchment area were also excluded (fp_frac < 20%). Finally, catchments showing signs of artificial regulation in their hydrographs were removed. Worth mentioning is that after each criterion mentioned above there is a parenthesis which followed the CAMELS-CL nomenclature. For instance, glaciar cover is catalogued as "lc_glacier" and large dams as "big_dam".

The chosen catchments have diverse characteristics, reflecting significant variability. For instance, the smallest catchment has a size of 35 km^2, whereas the largest one has a size of 11,137 km^2 (median catchment size is 672 km^2). In terms of mean annual precipitation, it ranges from 94 to 3,660 mm/year (median value of 1,393 mm/year). The aridity index also covers a wide spectrum of values, ranging from 0.3 (Southern Chile) to 31.6 (Northern Chile). Its median is 0.69. In terms of mean elevations, they range between 118 (western, Pacific Ocean) and 4,270 (eastern, Andes Mountains) meters above sea level (m.a.s.l.). They have a median elevation of 1,052 m.a.s.l.. In terms of seasonality, winter rainfall predominates with a few exceptions in Northern catchments where precipitation is concentrated during the summer (Garreaud, 2009). Additionally, precipitation usually increases from north to south while temperatures decrease (Sarricolea et al., 2017).

https://doi.org/10.5194/hess-2024-389
Preprint. Discussion started: 21 January 2025
© Author(s) 2025. CC BY 4.0 License.
Hydrology and Earth System Sciences
Discussions

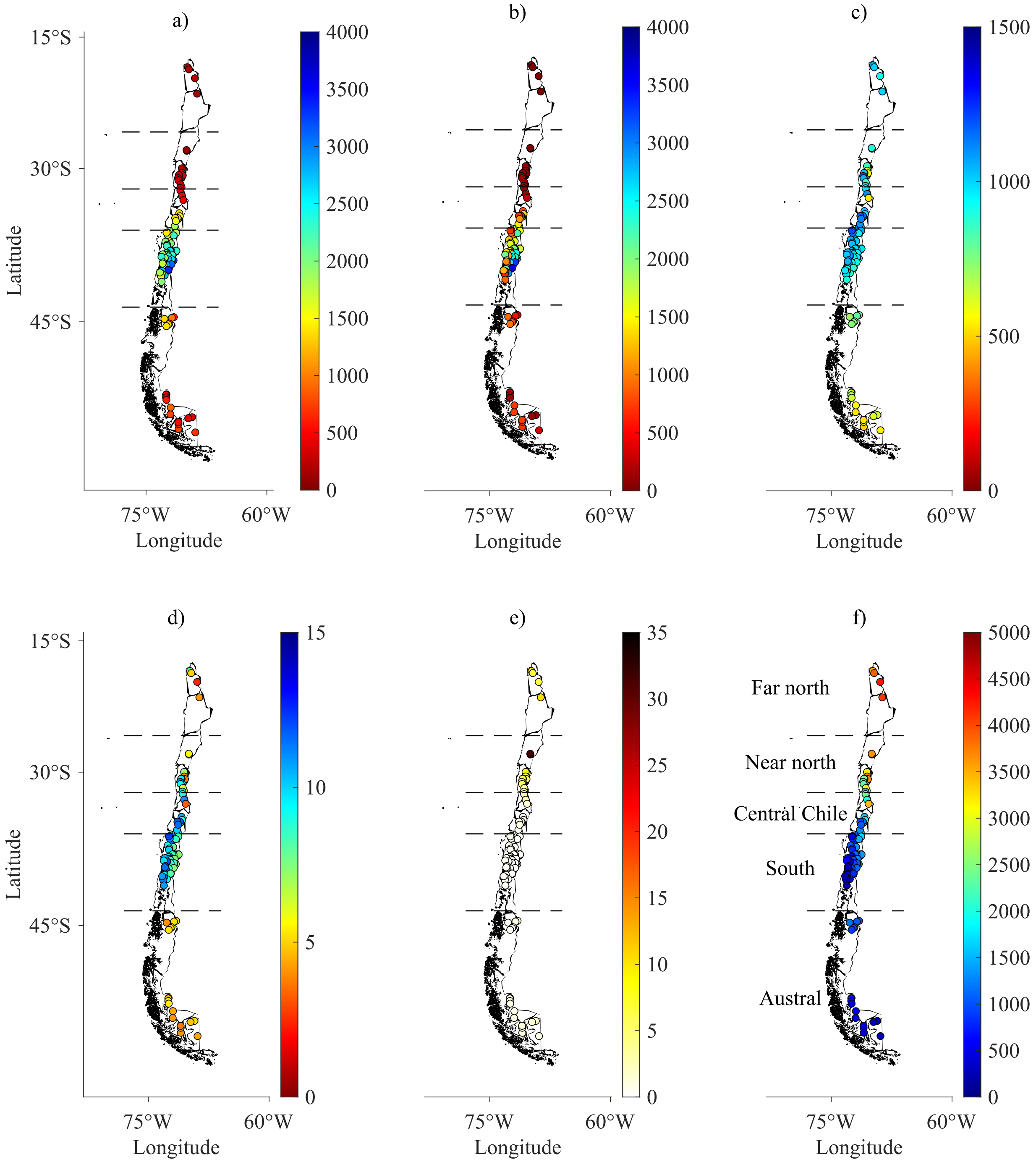

125 **Figure 1: Locations and characteristics of analysed catchments. Coloured dots represent the catchment outlet locations. Five zones are explicitly presented on the right to highlight differences of catchment climatic characteristics. From a) to c), mean annual**

https://doi.org/10.5194/hess-2024-389
Preprint. Discussion started: 21 January 2025
© Author(s) 2025. CC BY 4.0 License.

precipitation, runoff, and potential evapotranspiration (all of them in [mm]). d) Mean annual temperature in [º C], e) Aridity index (dimensionless), and, f) Catchment outlet elevations in [m].

2.3 Uncertainty consideration, entropy-based concepts, and RUMI formulation

2.3.1 BLUECAT

Koutsoyiannis and Montanari (2022) proposed BLUECAT with the intention to transform a deterministic prediction model into a stochastic one. BLUECAT's predecessor was introduced by Montanari and Koutsoyiannis (2012). BLUECAT transforms deterministic simulations into stochastic simulations (with confidence bands). Unlike deterministic predictions, the confidence band represents a range of possible outcomes, allowing to consider the stochastic result as a representative value of the sample (such as the mean or median). Worth mentioning is that uncertainty can be quantified as well. We use BLUECAT to transform deterministic rainfall-runoff simulations to stochastic ones to consider uncertainty quantification in model calibration.

BLUECAT's flowchart starts with a deterministic simulation and identifies the simulated variable (streamflow in our case) at each time point. For each point, a sample is established comprising neighbouring simulated river flows, defined by m_1 flows smaller and m_2 flows larger than the point's discharge, both with the smallest differences. The observed data corresponding to these simulated flows forms a sample of streamflow values. The latter is happening at each time point. An empirical distribution function of this sample is then used to estimate uncertainty for a given confidence level, using the mean or median as representative results of the stochastic simulation. Alternative methods, such as the ones using a theoretical probability distribution can also manage the sample (e.g., Pareto-Burr-Feller with knowable moments). In this work, BLUECAT is used with empirical computations with the intention to avoid any additional assumption. Worth mentioning is that BLUECAT allows uncertainty quantification through a proper uncertainty measure. Montanari and Koutsoyiannis (2024) proposed 4 measures basing on the distance between the confidence bands, for a given significance level, and the mean value of the prediction.

BLUECAT was originally implemented in R (coupled with the HyMod rainfall-runoff model, Koutsoyiannis and Montanari 2022) and recently, Montanari and Koutsoyiannis (2024) made available BLUECAT with multimodel usage in R and Python. Codes in Matlab are also available (see Jorquera and Pizarro 2023)

2.3.2 RUMI: Ratio of Uncertainty to Mutual Information

In information theory, the entropy of a random variable is a measure of its uncertainty or the measure of the information amount required, on average, to describe the random variable itself (Thomas and Joy, 2006). The amount of information one random variable contains about another random variable is usually defined as mutual information (MI). MI is, indeed, the reduction of one random variable uncertainty due to the knowledge of the other. MI can be defined as a function of marginal $\left(H(\underline{Y})\right)$ and conditional entropies $\left(H(\underline{Y}/\underline{X})\right)$:

https://doi.org/10.5194/hess-2024-389
Preprint. Discussion started: 21 January 2025
© Author(s) 2025. CC BY 4.0 License.

$$\mathrm{MI}(\underline{Y}, \underline{X}) = H(\underline{Y}) - H(\underline{Y}/\underline{X}), \tag{1}$$

where $H(\underline{Y}) = -E[\log(p(Y))]$, $H(\underline{Y}/\underline{X}) = -E[\log(p(Y/X))]$, $p(\alpha)$ is the probability mass function of a random variable $\underline{\alpha}$ (or the probability density if the variable is of continuous type), and $E[\quad]$ denotes expectation. Note that random variables are underlined, following the Dutch convention (Hemelrijk, 1966).

Additionally, the normalised mutual information (also called as uncertainty coefficient, entropy coefficient, or Theil's U) can be computed as:

$$U(\underline{Y}, \underline{X}) = \frac{\mathrm{MI}(\underline{Y}, \underline{X})}{H(\underline{Y})} = \frac{H(\underline{Y}) - H(\underline{Y}/\underline{X})}{H(\underline{Y})}. \tag{2}$$

Taking $\underline{Y}$ as the observed streamflow $\left(\underline{Q_{\mathrm{obs}}}\right)$ and $\underline{X}$ as the simulated one with BLUECAT ($\underline{Q_{\mathrm{sim}}}$, given by the mean value of the distribution of the predictand), $U(\underline{Y}, \underline{X}) = U\left(\underline{Q_{\mathrm{obs}}}, \underline{Q_{\mathrm{sim}}}\right)$ represents the normalised amount of information that $\underline{Q_{\mathrm{sim}}}$ contains about $\underline{Q_{\mathrm{obs}}}$. Note that $\underline{Q_{\mathrm{sim}}}$ can also be estimated by the median value of the distribution of the predictand (or another quantile). The decision of using the mean value relies on Jorquera and Pizarro (2023) results that showed higher KGE values using the mean than the median value for all analysed catchments.

Furthermore, a proper uncertainty measure of the stochastic model computed with BLUECAT can be defined as the width of the confidence limits divided by its mean value and averaged through the whole simulation period, i.e.:

$$u = \sum_{\tau=1}^{n} \frac{1}{n} \left| \frac{Q_{\tau,u} - Q_{\tau,l}}{Q_{\tau,\mathrm{sim}}} \right|, \tag{3}$$

where $Q_{\tau,u} - Q_{\tau,l}$ are the upper and lower confidence limits for the streamflow stochastic prediction at time step τ, $Q_{\tau,\mathrm{sim}}$ is its mean value at time step τ, and n is the total number of time steps.

Notice that both u and $U\left(\underline{Q_{\mathrm{obs}}}, \underline{Q_{\mathrm{sim}}}\right)$ are dimensionless quantities and, in ideal conditions, it is desirable that u is minimised (i.e., low uncertainty), whereas $U\left(\underline{Q_{\mathrm{obs}}}, \underline{Q_{\mathrm{sim}}}\right)$ is maximised (i.e., high mutual information between simulated and observed stream flows). Therefore, the ratio between u and $U\left(\underline{Q_{\mathrm{obs}}}, \underline{Q_{\mathrm{sim}}}\right)$ gives a measure of the simulation performance. Worth to mention is that the advantage of taking this ratio does not only rely on a mathematical desire (i.e., the ratio should be minimised in calibration) but on the fact that it is possible to have narrow confidence limits (i.e., low uncertainty) with a bad performance between the stochastic model predictand and observed values (i.e., low mutual information. See Fig. 2a). Additionally, it is also possible to have high mutual information (stochastic model predictand close to observed values) but with high uncertainty as shown in Fig. 2b. Therefore, taking the ratio is twofold: i) mathematical desire (i.e., optimisation); and, ii) deductive conceptual reasoning. As a consequence, and with the intention to provide a metric ranging between 0 and 1, the **R**atio of **U**ncertainty to **M**utual **I**nformation (**RUMI**) is presented:

$$\mathrm{RUMI} = \frac{1}{1+\phi} = \frac{1}{1+\frac{u}{U\left(\underline{Q_{\mathrm{obs}}}, \underline{Q_{\mathrm{sim}}}\right)}}. \tag{4}$$

https://doi.org/10.5194/hess-2024-389
Preprint. Discussion started: 21 January 2025
© Author(s) 2025. CC BY 4.0 License.

Notice that RUMI follows common-efficiency notions (i.e., perfect simulation means the highest metric value). Figure 2d shows the core steps of RUMI computation, whereas codes for RUMI are also available within this manuscript in Matlab and R (see Code and Results Availability statement).

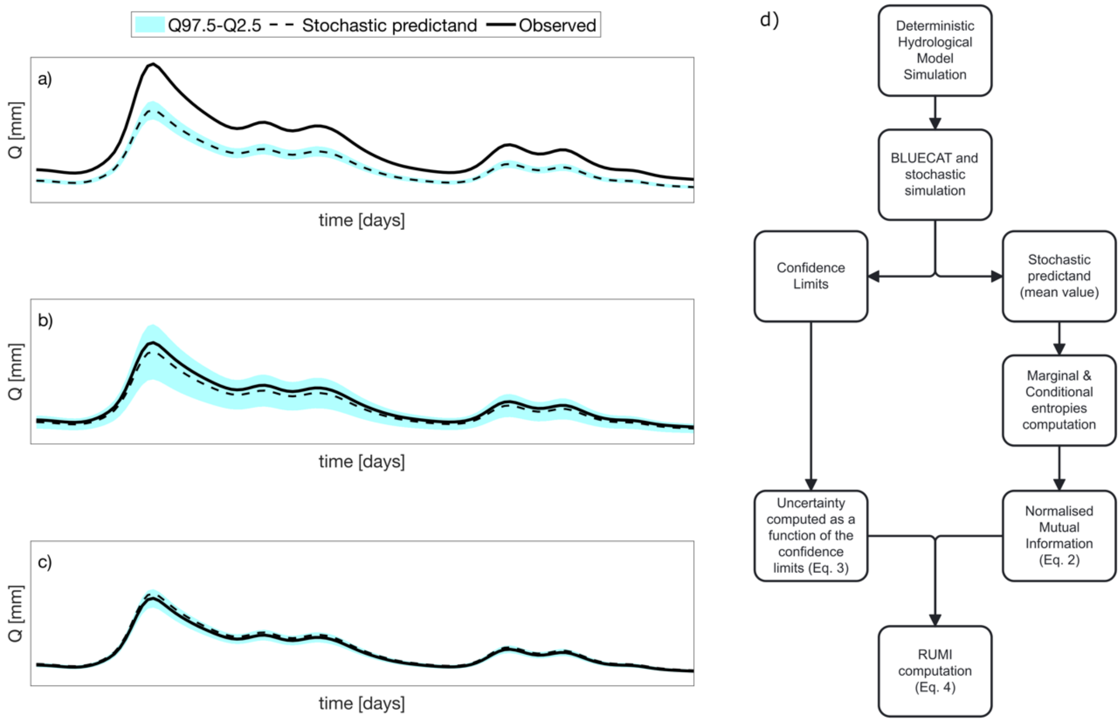

Figure 2: Illustration of possible modelling scenarios: a) low uncertainty and low mutual information (i.e., low RUMI value); b) high uncertainty and high mutual information (i.e., low RUMI value); and, c) low uncertainty and high mutual information (i.e., high RUMI value). d) Flowchart of RUMI computation. Marginal and conditional entropies are computed empirically with bins. The filled cyan band is the area between the 97.5 and 2.5 percentiles of simulation estimated by BLUECAT.

2.4 Methodology Outline Summary

The methodology employed in this study involves the use of the GR4J hydrological model, implemented within the MARRMoT toolbox. The model is driven by daily precipitation and potential evapotranspiration data from the CAMELS-CL database, with the primary output being simulated daily streamflow. The analysis focuses on the period from 1990 to 2018, with a warm-up phase from 1990 to 1992, a calibration phase from 1992 to 2005, and a validation phase from 2005 to 2018. 99 catchments and five macroclimatic zones are covered (See Fig. 1).

Catchments were calibrated with two different objective functions: KGE and RUMI. KGE (Kling et al., 2012) – computed in this study with Eq. (5) – is the modified version of the KGE proposed initially by Gupta et al. (2009):

$$\mathrm{KGE} = 1 - \sqrt{\left(\frac{\mu_s}{\mu_o} - 1\right)^2 + \left(\frac{(\sigma_s/\mu_s)}{(\sigma_o/\mu_o)} - 1\right)^2 + (\rho - 1)^2}, \tag{5}$$

https://doi.org/10.5194/hess-2024-389
Preprint. Discussion started: 21 January 2025
© Author(s) 2025. CC BY 4.0 License.

where, μ_s is the mean value of deterministic streamflow simulations; μ_o is the mean value of streamflow observations; σ_s is the standard deviation of deterministic streamflow simulations; σ_o is the standard deviation of streamflow observations; and, ρ is the Pearson correlation coefficient between observed and deterministic simulation of streamflow.

Four additional metrics were used to assess performance of results: i) Nash-Sutcliffe Efficiency (NSE); ii) KGE knowable moments (KGEkm, Pizarro and Jorquera 2024); iii) Normalised Root Mean Squared Error (NRMSE); and, iv) Mean Absolute Relative Error (MARE). Equations for NSE, KGEkm, NRMSE, and MARE are presented from Eq. (6) to Eq. (9):

$$\mathrm{NSE} = 1 - \frac{\sum_{i=1}^{n}(O_i - S_i)^2}{\sum_{i=1}^{n}(O_i - \mu_o)^2}, \quad (6)$$

$$\mathrm{KGEkm} = 1 - \sqrt{\left(\frac{\mathrm{K}_{1_s}}{\mathrm{K}_{1_o}} - 1\right)^2 + \left(\frac{\left(\sqrt{\mathrm{K}_{2_s}}/\mathrm{K}_{1_s}\right)}{\left(\sqrt{\mathrm{K}_{2_o}}/\mathrm{K}_{1_o}\right)} - 1\right)^2 + (\rho - 1)^2}, \quad (7)$$

$$\mathrm{NRMSE} = \frac{\sqrt{\frac{1}{n}\left(\sum_{i=1}^{n}(S_i - O_i)^2\right)}}{\max(O) - \min(O)}, \quad (8)$$

$$\mathrm{MARE} = \frac{\sum_{i=1}^{n}\left|\frac{(S_i - O_i)}{O_i}\right|}{n}, \quad (9)$$

where, K_{1_s} and K_{1_o} are the first knowable moment of simulated and observed streamflow time series, and K_{2_s} and K_{2_o} are dispersion relying on the second knowable moments of simulated and observed streamflow time series. Notice that the square operator in K_2 is not necessary in Eq. (7) but intentionally used to be in line with classical statistics and KGE formulation (see Eq. 5). S and O mean simulated and observed streamflow time series, respectively. n is the length of the analysed period (at daily scale). RMSE, NRMSE and MARE have 0 at the perfect ideal value, whereas their values range from 0 to positive infinite. NSE and KGEkm have a range from minus infinite to 1, being 1 the ideal value.

Additionally, and with a particular focus on different runoff characteristics, 50 hydrological signatures were computed. Observed runoff, simulations with model calibrated with KGE, and simulations with model calibrated with RUMI were considered. Hydrological signatures were computed with the Toolbox for Streamflow Signatures in Hydrology (TOSSH, Gnann et al. (2021)). Table 1 shows the 50 computed signatures.

https://doi.org/10.5194/hess-2024-389
Preprint. Discussion started: 21 January 2025
© Author(s) 2025. CC BY 4.0 License.
Hydrology and Earth System Sciences
Open Access
EGU
Discussions

Table 1: 50 hydrological signatures computed with the Toolbox for Streamflow Signatures in Hydrology (TOSSH). The computed hydrological signatures follow TOSSH nomenclature (e.g., TotalRR is the total runoff ratio). A description of the signatures is also included.

Nº	Hydrological signature (using TOSSH nomenclature)	Description
1	Q_mean	Mean streamflow
2	TotalRR	Total runoff ratio
3	QP_elasticity	Streamflow-precipitation elasticity
4	FDC_slope	Slope of the flow duration curve
5	BFI	Baseflow index
6	HFD_mean	Half flow date
7	Q5	5th streamflow percentile
8	Q95	95th streamflow percentile
9	high_Q_freq	High flow frequency
10	high_Q_dur	High flow duration
11	low_Q_freq	Low flow frequency
12	low_Q_dur	Low flow duration
13	AC1	Lag-1 autocorrelation
14	AC1_low	Lag-1 autocorrelation for low flow period
15	RLD	Rising limb density
16	PeakDistribution	Slope of distribution of peaks
17	PeakDistribution_low	Slope of distribution of peaks for low flow period
18	IE_effect	Infiltration excess importance
19	SE_effect	Saturation excess importance
20	IE_thresh_signif	Infiltration excess threshold significance (in a plot of quickflow volume vs. maximum intensity)
21	SE_thresh_signif	Saturation excess threshold significance (in a plot of quickflow volume vs. total precipitation)
22	IE_thresh	Infiltration excess threshold location (in a plot of quickflow volume vs. maximum intensity)
23	SE_thresh	Saturation excess threshold location (in a plot of quickflow volume vs. total precipitation)
24	SE_slope	Saturation excess threshold above-threshold slope (in a plot of quickflow volume vs. total precipitation)

https://doi.org/10.5194/hess-2024-389
Preprint. Discussion started: 21 January 2025
© Author(s) 2025. CC BY 4.0 License.

25	Storage_thresh_signif	Storage/saturation excess threshold significance (in a plot of quickflow volume vs. antecedent precipitation index + total precipitation)
26	Storage_thresh	Storage/saturation excess threshold location (in a plot of quickflow volume vs. antecedent precipitation index + total precipitation)
27	min_Qf_perc	Minimum quickflow as a percentage of precipitation
28	EventRR	Event runoff ratio
29	RR_Seasonality	Runoff ratio seasonality
30	Recession_a_Seasonality	Seasonal variations in recession parameters
31	AverageStorage	Average storage from average baseflow and storage-discharge relationship
32	MRC_num_segments	Number of different segments in master recession curve (MRC)
33	BaseflowRecessionK	Exponential recession constant
34	First_Recession_Slope	Steep section of MRC = storage that is quickly depleted
35	Spearmans_rho	Non-uniqueness in the storage-discharge relationship
36	EventRR_TotalRR_ratio	Ratio between event and total runoff ratio
37	VariabilityIndex	Variability index of flow
38	BaseflowMagnitude	Difference between maximum and minimum of annual baseflow regime
39	FlashinessIndex	Richards-Baker flashiness idex
40	HFI_mean	Half flow interval
41	Q_CoV	Coefficient of variation
42	Q_mean_monthly	Mean monthly streamflow
43	Q_7_day_max	7-day maximum streamflow
44	Q_7_day_min	7-day minimum streamflow
45	Q_skew	Skewness of streamflow
46	Q_var	Variance of streamflow
47	RecessionK_part	Recession constant of early/late (exponential) recessions
48	ResponseTime	Catchment response time
49	SnowStorage	Snow storage derived from cumulative P-Q regime curve

https://doi.org/10.5194/hess-2024-389
Preprint. Discussion started: 21 January 2025
© Author(s) 2025. CC BY 4.0 License.

50	StorageFromBaseflow	Average storage from average baseflow and storage-discharge relationship

3 Results

Fig. 3 shows a graphical example of RUMI-based hydrological modelling of two of the catchments in calibration (Fig. 3a, catchment number: 8123001) and validation (Fig. 3b, catchment number: 9437002) over the years 1996 and 2016, respectively. Additionally, it shows observed and simulated stream flows, which were calibrated with KGE (red continuous line) and RUMI (blue continuous line is the mean of the stochastic simulation). 97.5 and 2.5 percentiles (computed with BLUECAT and RUMI) are shown with a violet band. Fig. 3a.2 and Fig. 3b.2 show observed and simulated stream flows over the complete period of analysis (performance of KGE-based simulations was 0.89 (0.80) and 0.95 (0.91) in calibration (validation) as well as the performance of RUMI-based simulations was 0.27 (0.20) and 0.46 (0.48) in calibration (validation), respectively). Worth to mention is that observed streamflow was between the 97.5 and 2.5 percentiles (i.e., the violet band) all the time except 4.93% and 0.19% of the time, presenting higher and lower observed streamflow, respectively (see, e.g., one event in June 1996 in Fig. 3a and one event in July 2016 in Fig. 3b).

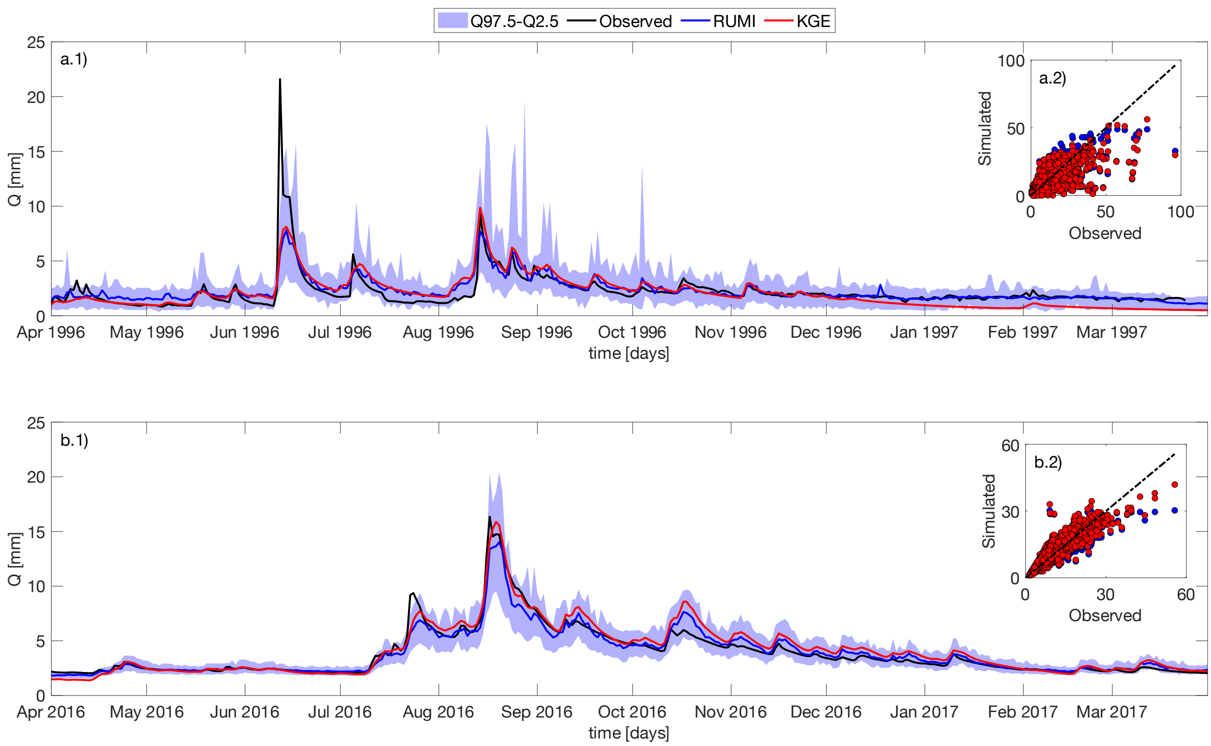

Figure 3: Observed and simulated stream flows for the hydrological year 1996-1997 (a) and 2016-2017 (b). a.1) Catchment ID: 8123001 in calibration; b.1) Catchment ID: 9437002 in validation. Black: observed streamflow; Red: simulated by the deterministic model calibrated with KGE; Blue: simulated with the model calibrated with RUMI (mean stochastic simulation).

https://doi.org/10.5194/hess-2024-389
Preprint. Discussion started: 21 January 2025
© Author(s) 2025. CC BY 4.0 License.

The filled violet band is the area between the 97.5 and 2.5 percentiles of simulation estimated by BLUECAT. The dashed line represents the perfect agreement between observed and simulated streamflow.

In terms of other performance metrics, Fig. 4 shows NSE (a.1, b.1), KGEkm (a.2, b.2), NRMSE (a.3, b.3), and MARE (a.4, b.4) in calibration (a.1, a.2, a.3, a.4) and validation (b.1, b.2, b.3, b.4). Red markers are outliers, and grey dots represent the mean values (as a function of RUMI- and KGE-based simulations) which are linked with a grey line.

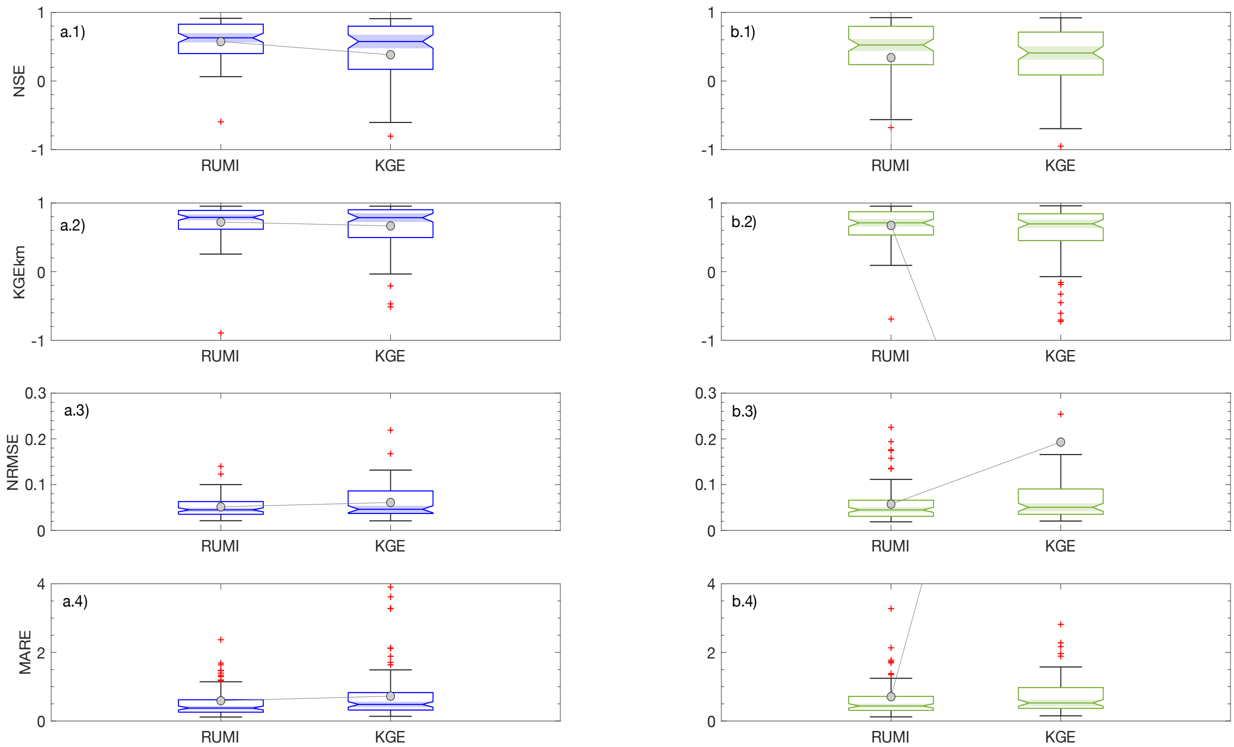

Figure 4: Performance metrics in calibration (a.1, a.2, a.3, a.4) and validation (b.1, b.2, b.3, b.4). Red markers denote outliers. Grey dots represent the mean values computed with RUMI and KGE, which are linked to grey lines. Note that the y-axis limits are truncated for visualisation purposes.

Remarkably, RUMI-based simulations outperform KGE-based ones in calibration and validation, and for the four performance metrics analysed. The latter in terms of variability (e.g., the interquartile range – IQR), median of boxplots, and number of outliers for both calibration and validation periods. Table 2 summarises the four considered performance metrics in terms of: a) calibration and validation; b) RUMI and KGE; and, c) minimum, maximum, median, IQR, and mean values.

https://doi.org/10.5194/hess-2024-389
Preprint. Discussion started: 21 January 2025
© Author(s) 2025. CC BY 4.0 License.
Hydrology and Earth System Sciences
Discussions

Table 2: Statistic's summary of boxplots results (see also Fig. 4).

		Calibration				Validation			
		NSE	KGEkm	NRMSE	MARE	NSE	KGEkm	NRMSE	MARE
Min	RUMI	-0.59	-0.89	0.02	0.12	-14.11	-0.69	0.02	0.12
	KGE	-1.80	-0.51	0.02	0.14	-299732	-616	0.02	0.15
Max	RUMI	0.91	0.95	0.14	7.81	0.92	0.95	0.23	5.56
	KGE	0.91	0.95	0.22	3.90	0.92	0.96	12.58	1755
Median	RUMI	0.63	0.79	0.04	0.38	0.53	0.71	0.04	0.44
	KGE	0.58	0.79	0.05	0.48	0.41	0.70	0.05	0.53
IQR	RUMI	0.43	0.27	0.03	0.36	0.56	0.34	0.04	0.41
	KGE	0.63	0.41	0.05	0.51	0.62	0.39	0.06	0.61
Mean	RUMI	0.57	0.72	0.05	0.59	0.34	0.67	0.06	0.71
	KGE	0.38	0.67	0.06	0.72	-3027	-5.67	0.19	18.76

Based on Fig. 4 and Table 2, RUMI-based simulations showed more stable and consistent performance than KGE in calibration and validation phases. While KGE can achieve high accuracy (see, e.g., the maximum value of NSE for RUMI and KGE), it exhibits more variability and more extreme outliers. The latter, particularly during validation, indicates a lack of robustness. On the other hand, RUMI presented lower variability, more consistent results, and the opportunity to consider the confidence intervales in calibration.

Table 3 shows the 50 computed hydrological signatures with a correlation comparison between simulations and observed hydrological signatures (green and red colours in Table 3 mean outperformance and underperformance, respectively). On average, RUMI outperforms KGE-based simulations (average values: 0.72 vs 0.48) and minimum and maximum values (-0.07 vs -0.10 and 1.00 vs 0.96, respectively). RUMI-based simulations outperform KGE-based ones by 82% of the considered hydrologic signatures. Fig. 5 shows four examples of this comparison in terms of the runoff ratio (TotalRR, Fig. 5a), streamflow-precipitation elasticity (QP_elasticity, Fig. 5b); 5-th flow percentile of streamflow (Q5, Fig. 5c), and 95-th flow percentile of streamflow (Q95, Fig. 5d). Colours of the dots are related to the five different defined macroclimatic zones depicted in Fig. 1.

https://doi.org/10.5194/hess-2024-389
Preprint. Discussion started: 21 January 2025
© Author(s) 2025. CC BY 4.0 License.
Hydrology and Earth System Sciences
Discussions
Open Access
EGU

265 **Table 3: 50 used hydrological signatures. Performance was assessed using Pearson's correlation coefficient. Hydrological signatures were computed with TOSSH. Colours were added to visually observe which objective function performed better (green means better than red). The average, minimum, and maximum values were computed and added at the end of the list.**

Hydrological signature	Obs versus KGE	Obs versus RUMI	Hydrological signature	Obs versus KGE	Obs versus RUMI
Q_mean	0.90	1.00	EventRR	0.96	0.98
TotalRR	-0.06	1.00	RR_Seasonality	0.83	0.86
QP_elasticity	0.30	0.63	Recession_a_Seasonality	0.20	0.37
FDC_slope	0.30	0.86	AverageStorage	0.72	0.87
BFI	0.74	0.83	MRC_num_segments	-0.10	-0.07
HFD_mean	0.75	0.94	BaseflowRecessionK	0.33	0.65
Q5	0.96	0.99	First_Recession_Slope	0.34	0.40
Q95	0.41	0.99	Spearmans_rho	0.48	0.65
high_Q_freq	0.52	0.91	EventRR_TotalRR_ratio	0.85	0.97
high_Q_dur	0.27	0.28	VariabilityIndex	0.06	0.91
low_Q_freq	0.56	0.95	BaseflowMagnitude	0.95	0.97
low_Q_dur	-0.09	0.61	FlashinessIndex	0.86	0.91
AC1	0.67	0.69	HFI_mean	0.63	0.86
AC1_low	0.61	0.59	Q_CoV	0.89	0.82
RLD	0.16	0.15	Q_mean_monthly	0.74	0.99
PeakDistribution	0.28	0.76	Q_7_day_max	0.77	0.94
PeakDistribution_low	0.07	0.57	Q_7_day_min	-0.04	0.95
IE_effect	0.53	0.51	Q_skew	0.45	0.58
SE_effect	0.68	0.67	Q_var	0.10	0.98
IE_thresh_signif	0.63	0.50	RecessionK_early	0.82	0.67
SE_thresh_signif	0.51	0.41	ResponseTime	0.42	0.25
IE_thresh	-0.04	0.53	SnowStorage	0.95	0.98
SE_thresh	-0.06	0.65	StorageFromBaseflow	0.79	0.84
SE_slope	0.71	0.72	**Average**	0.48	0.72
Storage_thresh_signif	0.49	0.53	**Min**	-0.10	-0.07
Storage_thresh	-0.04	0.70	**Max**	0.96	1.00
min_Qf_perc	-0.02	0.63			

https://doi.org/10.5194/hess-2024-389
Preprint. Discussion started: 21 January 2025
© Author(s) 2025. CC BY 4.0 License.

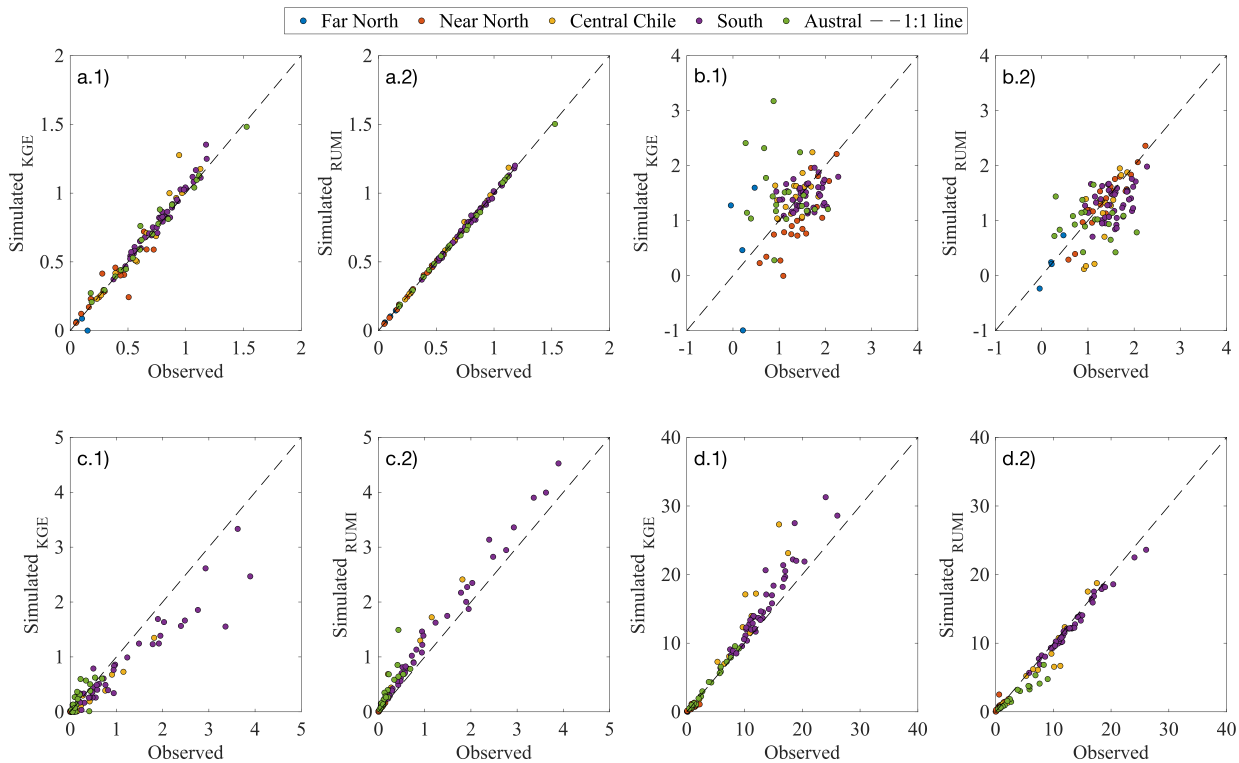

Figure 5: Observed and simulated hydrological signatures (only for illustration purposes) for each case (a.1, b.1, c.1, d1: simulated with KGE; and, a.2, b.2, c.2, d.2: simulated with RUMI). a: runoff ratio (TotalRR); b: streamflow-precipitation elasticity (QP_elasticity); c: 5-th flow percentile of streamflow (Q5); d: 95-th flow percentile of streamflow (Q95). Colours of dots are related to the five considered macroclimatic zones. The dashed line represents the perfect agreement between observed and simulated hydrological signature. Note that the y-axis limits for the a.1 plot are truncated for visualisation purposes (original y-axis range: [0, 30]).

4 Strengths and limitations

The proposed approach provides a comprehensive measure of the shared information between observed and simulated stream flows, normalises this measure for comparability, and integrates uncertainty quantification in the calibration process. The rescaling of the performance metric ensures intuitive interpretation, aligning with standard efficiency metrics and making it easy to understand. Additionally, this research analysed 99 catchments in a pseudo-natural hydrologic regime that covers different macroclimatic zones and, therefore, giving robustness to the analysis. The latter ensures a diverse representation of hydrological characteristics and a broad evaluation of the RUMI-based modelling approach. The simplicity of the approach, its capacity to quantify confidence intervals and, therefore, also uncertainty quantification are significant strengths. As demonstrated by the IQR, the median of results, and outliers (see Table 2), simulations during validation are

© Author(s) 2025. CC BY 4.0 License.

also seen to improve. Also, using the 50 hydrological signatures, the RUMI-based approach was compared considering different runoff dynamics characteristics showing improvements for most. RUMI-based performances rely on the combination of available information (in terms of observed quantities) and physically based consistency of modelled hydrological processes (BLUECAT alongside entropy-based computations and deterministic rainfall-runoff model). RUMI-based modelling implementation is also facilitated by the codes provided in this manuscript (see Code and Results availability statement), which enhances the reproducibility of the methodology.

RUMI considers uncertainty quantification in its computing process and, therefore, we emphasise the fact that other methodologies for such purposes should be testing (such as multi-model ensemble methods or time-varying model parameters. See Gupta and Govindaraju 2023 for a recent review in this regard). The latter with the intention to quantify the metric uncertainty. Additionally, RUMI calculations can be computationally intensive. The method's accuracy depends on high-quality input data and length of the time series (BLUECAT assumes that the calibration dataset is extended enough to upgrade from the deterministic to the stochastic model). It also assumes that observed and simulated stream flows can be effectively described by these measures, which may not capture all dependencies and non-linearities. Finally, entropy and mutual information might be sensitive to outliers.

5 Conclusions

The RUMI-based hydrological modelling approach outperforms KGE-based modelling in both calibration and validation phases across various performance metrics. This method demonstrates lower variability and a consistent performance improvement. RUMI's capability to quantify uncertainty and incorporate it into the calibration process ensure more reliable predictions. The analysis of hydrological signatures further confirms the superiority of RUMI, with 82% of the signatures showing a better correlation with observed data compared to KGE. RUMI offers a valuable tool for hydrological modelling, enhancing the understanding and prediction of streamflow under different hydrological conditions.

Possible additional research is mentioned as follows: (a) Testing the RUMI-based approach with other rainfall-runoff models (lumped, semi-distributed, and distributed hydrological models); (b) Testing the RUMI-based approach under other hydroclimatological catchment characteristics and in a higher number of catchments; (c) Testing alternative uncertainty quantification methods; (d) Exploring the impact of varying data quality on RUMI performance to establish guidelines for data requirements; and, (e) Exploring the applicability of the RUMI in other disciplines such as meteorology, environmental science, and ecology where modelling and uncertainty quantification are critical.

https://doi.org/10.5194/hess-2024-389
Preprint. Discussion started: 21 January 2025
© Author(s) 2025. CC BY 4.0 License.

Code and Data availability

RUMI codification – in Matlab and R – is available in Pizarro et al. (2024): https://www.doi.org/10.17605/OSF.IO/93N4R. Data used in this study are available in the CAMELS-CL dataset (Alvarez-Garreton et al., 2018): https://doi.pangaea.de/10.1594/PANGAEA.894885

Author contribution

AM and DK developed the BLUECAT code in R. AP developed RUMI codes and performed simulations. AP prepared the manuscript with contributions from all co-authors.

Competing Interest

The authors declare that they have no conflict of interest.

Financial support

AP was supported by The National Research and Development Agency of the Chilean Ministry of Science, Technology, Knowledge and Innovation (ANID), grant no. FONDECYT Iniciación 11240171. AM was partially supported by (1) the RETURN Extended Partnership which received funding from the European Union Next-GenerationEU (National Recovery and Resilience Plan – NRRP, Mission 4, Component 2, Investment 1.3 – D.D. 1243 2/8/2022, PE0000005) and (2) the Italian Science Fund through the project "Stochastic amplification of climate change into floods and droughts change (CO$_2$2Water)", grant number J53C23003860001. DK was not supported at all.

References

Alvarez-Garreton, C., Mendoza, P. A., Boisier, J. P., Addor, N., Galleguillos, M., Zambrano-Bigiarini, M., Lara, A., Puelma, C., Cortes, G., and Garreaud, R.: The CAMELS-CL dataset: catchment attributes and meteorology for large sample studies–Chile dataset, Hydrology and Earth System Sciences, 22, 5817–5846, 2018.

Amorocho, J. and Espildora, B.: Entropy in the assessment of uncertainty in hydrologic systems and models, Water Resources Research, 9, 1511–1522, 1973.

Auer, A., Gauch, M., Kratzert, F., Nearing, G., Hochreiter, S., and Klotz, D.: A data-centric perspective on the information needed for hydrological uncertainty predictions, Hydrology and Earth System Sciences, 28, 4099–4126, https://doi.org/10.5194/hess-28-4099-2024, 2024.

Beven, K.: Prophecy, reality and uncertainty in distributed hydrological modelling, Advances in water resources, 16, 41–51, 1993.

Beven, K.: A manifesto for the equifinality thesis, Journal of Hydrology, 320, 18–36, https://doi.org/10.1016/j.jhydrol.2005.07.007, 2006.

Beven, K.: A brief history of information and disinformation in hydrological data and the impact on the evaluation of hydrological models, Hydrological Sciences Journal, 69, 519–527, 2024.

Beven, K. and Binley, A.: The future of distributed models: model calibration and uncertainty prediction, Hydrological processes, 6, 279–298, 1992.

Blasone, R.-S., Vrugt, J. A., Madsen, H., Rosbjerg, D., Robinson, B. A., and Zyvoloski, G. A.: Generalized likelihood uncertainty estimation (GLUE) using adaptive Markov Chain Monte Carlo sampling, Advances in Water Resources, 31, 630–648, https://doi.org/10.1016/j.advwatres.2007.12.003, 2008.

Blazkova, S. and Beven, K.: Flood frequency estimation by continuous simulation for a catchment treated as ungauged (with uncertainty), Water Resources Research, 38, 14-1-14–14, https://doi.org/10.1029/2001WR000500, 2002.

Blazkova, S. and Beven, K.: Flood frequency estimation by continuous simulation of subcatchment rainfalls and discharges with the aim of improving dam safety assessment in a large basin in the Czech Republic, Journal of Hydrology, 292, 153–172, 2004.

Blöschl, G., Bierkens, M. F., Chambel, A., Cudennec, C., Destouni, G., Fiori, A., Kirchner, J. W., McDonnell, J. J., Savenije, H. H., and Sivapalan, M.: Twenty-three unsolved problems in hydrology (UPH)–a community perspective, Hydrological sciences journal, 64, 1141–1158, 2019.

Chapman, T. G.: Entropy as a measure of hydrologic data uncertainty and model performance, Journal of Hydrology, 85, 111–126, 1986.

Christensen, S.: A synthetic groundwater modelling study of the accuracy of GLUE uncertainty intervals, Hydrology Research, 35, 45–59, 2004.

Garreaud, R.: The Andes climate and weather, Advances in Geosciences, 22, 3–11, 2009.

Gnann, S. J., Coxon, G., Woods, R. A., Howden, N. J. K., and McMillan, H. K.: TOSSH: A Toolbox for Streamflow Signatures in Hydrology, Environmental Modelling & Software, 138, 104983, https://doi.org/10.1016/j.envsoft.2021.104983, 2021.

Gong, W., Gupta, H. V., Yang, D., Sricharan, K., and Hero III, A. O.: Estimating epistemic and aleatory uncertainties during hydrologic modeling: An information theoretic approach, Water Resources Research, 49, 2253–2273, https://doi.org/10.1002/wrcr.20161, 2013.

Gong, W., Yang, D., Gupta, H. V., and Nearing, G.: Estimating information entropy for hydrological data: One-dimensional case, Water Resources Research, 50, 5003–5018, https://doi.org/10.1002/2014WR015874, 2014.

Gupta, A. and Govindaraju, R. S.: Uncertainty quantification in watershed hydrology: Which method to use?, Journal of Hydrology, 616, 128749, https://doi.org/10.1016/j.jhydrol.2022.128749, 2023.

Gupta, H. V., Kling, H., Yilmaz, K. K., and Martinez, G. F.: Decomposition of the mean squared error and NSE performance criteria: Implications for improving hydrological modelling, Journal of Hydrology, 377, 80–91, https://doi.org/10.1016/j.jhydrol.2009.08.003, 2009.

https://doi.org/10.5194/hess-2024-389
Preprint. Discussion started: 21 January 2025
© Author(s) 2025. CC BY 4.0 License.

Hansen, N. and Ostermeier, A.: Adapting arbitrary normal mutation distributions in evolution strategies: The covariance matrix adaptation, Proceedings of IEEE international conference on evolutionary computation, 312–317, 1996.

Hansen, N., Müller, S. D., and Koumoutsakos, P.: Reducing the time complexity of the derandomized evolution strategy with covariance matrix adaptation (CMA-ES), Evolutionary computation, 11, 1–18, 2003.

Hemelrijk, J.: Underlining random variables, Statistica Neerlandica, 20, 1–7, 1966.

Jorquera, J. and Pizarro, A.: Unlocking the potential of stochastic simulation through Bluecat: Enhancing runoff predictions in arid and high-altitude regions, Hydrological Processes, 37, e15046, https://doi.org/10.1002/hyp.15046, 2023.

Kennedy, M. C. and O'Hagan, A.: Bayesian calibration of computer models, Journal of the Royal Statistical Society: Series B (Statistical Methodology), 63, 425–464, 2001.

Kling, H., Fuchs, M., and Paulin, M.: Runoff conditions in the upper Danube basin under an ensemble of climate change scenarios, Journal of Hydrology, 424–425, 264–277, https://doi.org/10.1016/j.jhydrol.2012.01.011, 2012.

Knoben, W. J. M., Freer, J. E., Fowler, K. J. A., Peel, M. C., and Woods, R. A.: Modular Assessment of Rainfall–Runoff Models Toolbox (MARRMoT) v1.2: an open-source, extendable framework providing implementations of 46 conceptual hydrologic models as continuous state-space formulations, Geoscientific Model Development, 12, 2463–2480, https://doi.org/10.5194/gmd-12-2463-2019, 2019.

Koutsoyiannis, D. and Montanari, A.: Bluecat: A local uncertainty estimator for deterministic simulations and predictions, Water Resources Research, 58, e2021WR031215, 2022a.

Koutsoyiannis, D. and Montanari, A.: Climate extrapolations in hydrology: the expanded BlueCat methodology, Hydrology, 9, 86, 2022b.

Krzysztofowicz, R.: Bayesian system for probabilistic river stage forecasting, Journal of hydrology, 268, 16–40, 2002.

Kuczera, G., Kavetski, D., Franks, S., and Thyer, M.: Towards a Bayesian total error analysis of conceptual rainfall-runoff models: Characterising model error using storm-dependent parameters, Journal of hydrology, 331, 161–177, 2006.

Mantovan, P. and Todini, E.: Hydrological forecasting uncertainty assessment: Incoherence of the GLUE methodology, Journal of hydrology, 330, 368–381, 2006.

Montanari, A.: Large sample behaviors of the generalized likelihood uncertainty estimation (GLUE) in assessing the uncertainty of rainfall-runoff simulations, Water resources research, 41, 2005.

Montanari, A. and Koutsoyiannis, D.: A blueprint for process-based modeling of uncertain hydrological systems, Water Resources Research, 48, 2012.

Montanari, A. and Koutsoyiannis, D.: Uncertainty estimation for environmental multimodel predictions: the BLUECAT approach and software, 18 September 2024.

Nash, J. E. and Sutcliffe, J. V.: River flow forecasting through conceptual models part I — A discussion of principles, Journal of Hydrology, 10, 282–290, https://doi.org/10.1016/0022-1694(70)90255-6, 1970.

© Author(s) 2025. CC BY 4.0 License.

Page, T., Smith, P., Beven, K., Pianosi, F., Sarrazin, F., Almeida, S., Holcombe, L., Freer, J., Chappell, N., and Wagener, T.: The CREDIBLE Uncertainty Estimation (CURE) toolbox: facilitating the communication of epistemic uncertainty, Hydrology and Earth System Sciences, 27, 2523–2534, 2023.

Pechlivanidis, I. G., Jackson, B., McMillan, H., and Gupta, H.: Use of an entropy-based metric in multiobjective calibration to improve model performance, Water Resources Research, 50, 8066–8083, https://doi.org/10.1002/2013WR014537, 2014.

Pechlivanidis, I. G., Jackson, B., Mcmillan, H., and Gupta, H. V.: Robust informational entropy-based descriptors of flow in catchment hydrology, Hydrological Sciences Journal, 61, 1–18, https://doi.org/10.1080/02626667.2014.983516, 2016.

Perrin, C., Michel, C., and Andréassian, V.: Improvement of a parsimonious model for streamflow simulation, Journal of hydrology, 279, 275–289, 2003.

Pizarro, A. and Jorquera, J.: Advancing objective functions in hydrological modelling: Integrating knowable moments for improved simulation accuracy, Journal of Hydrology, 634, 131071, https://doi.org/10.1016/j.jhydrol.2024.131071, 2024.

Rozos, E., Koutsoyiannis, D., and Montanari, A.: KNN vs. Bluecat—Machine learning vs. classical statistics, Hydrology, 9, 101, 2022.

Ruddell, B. L., Drewry, D. T., and Nearing, G. S.: Information Theory for Model Diagnostics: Structural Error is Indicated by Trade-Off Between Functional and Predictive Performance, Water Resources Research, 55, 6534–6554, https://doi.org/10.1029/2018WR023692, 2019.

Sarricolea, P., Herrera-Ossandon, M., and Meseguer-Ruiz, Ó.: Climatic regionalisation of continental Chile, Journal of Maps, 13, 66–73, https://doi.org/10.1080/17445647.2016.1259592, 2017.

Shannon, C. E.: A mathematical theory of communication, The Bell system technical journal, 27, 379–423, 1948.

Sikorska, A. E., Montanari, A., and Koutsoyiannis, D.: Estimating the uncertainty of hydrological predictions through data-driven resampling techniques, J. Hydrol. Eng, 20, A4014009, 2015.

Stedinger, J. R., Vogel, R. M., Lee, S. U., and Batchelder, R.: Appraisal of the generalized likelihood uncertainty estimation (GLUE) method, Water Resources Research, 44, https://doi.org/10.1029/2008WR006822, 2008.

Thomas, M. and Joy, A. T.: Elements of information theory, Wiley-Interscience, 2006.

Trotter, L., Knoben, W. J. M., Fowler, K. J. A., Saft, M., and Peel, M. C.: Modular Assessment of Rainfall–Runoff Models Toolbox (MARRMoT) v2.1: an object-oriented implementation of 47 established hydrological models for improved speed and readability, Geoscientific Model Development, 15, 6359–6369, https://doi.org/10.5194/gmd-15-6359-2022, 2022.

Vrugt, J. A., Ter Braak, C. J., Clark, M. P., Hyman, J. M., and Robinson, B. A.: Treatment of input uncertainty in hydrologic modeling: Doing hydrology backward with Markov chain Monte Carlo simulation, Water Resources Research, 44, 2008.

Weijs, S. V., Van Nooijen, R., and Van De Giesen, N.: Kullback–Leibler divergence as a forecast skill score with classic reliability–resolution–uncertainty decomposition, Monthly Weather Review, 138, 3387–3399, 2010a.

Weijs, S. V., Schoups, G., and van de Giesen, N.: Why hydrological predictions should be evaluated using information theory, Hydrology and Earth System Sciences, 14, 2545–2558, https://doi.org/10.5194/hess-14-2545-2010, 2010b.